THE JOURNAL OF PHYSICAL CHEMISTRY B

Article

pubs.acs.org/JPCB

Contributions of Far-Field Hydrodynamic Interactions to the Kinetics of Electrostatically Driven Molecular Association

Maciej Długosz,*[,†] Jan M. Antosiewicz,[‡] Paweł Zieliński,[§,∥,⊥] and Joanna Trylska[∥]

[†]Centre of New Technologies, [‡]Department of Biophysics, Faculty of Physics, [§]Interdisciplinary Centre for Mathematical and Computational Modeling, and [∥]Centre of New Technologies, University of Warsaw, Żwirki i Wigury 93, 02-089 Warsaw, Poland

[⊥]Department of Electronics and Information Technology, Institute of Electronic Systems, Warsaw University of Technology, Nowowiejska 15/19, 00-665 Warsaw, Poland

ABSTRACT: We simulated the diffusional encounters in periodic systems of model isotropic and anisotropic molecules using Brownian dynamics. We considered the electrostatic, excluded volume, and far-field hydrodynamic forces between diffusing molecules. Our goal was to estimate to what extent the hydrodynamic interactions influence the association kinetics when the associating partners are oppositely charged and their direct electrostatic interactions are screened by small mobile ions of dissolved salt. Overall, including hydrodynamic interactions decreases the association rate constants. The relative magnitude of this decrease does not depend on the ionic strength for the association of isotropic charged objects. This also holds true for nonspecific association (i.e., without restrictions regarding the relative orientation of binding partners in an encounter complex) of anisotropic objects. However, such dependence is visible for orientation-specific association of anisotropic objects. Moreover, we observe that some orientations of anisotropic molecules are hydrodynamically favorable during their mutual approach, and that such molecules can be hydrodynamically steered toward a particular relative orientation. This hydrodynamic orientational steering is impeded in case of strong electrostatic interactions or steric hindrance.

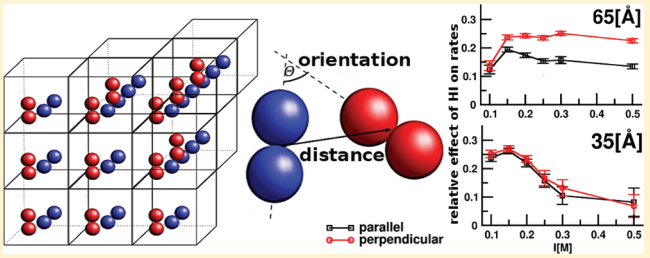

INTRODUCTION

Diffusional encounter of molecules is a first stage of many biologically relevant processes. Moreover, diffusion of molecules toward the encounter is often the rate-limiting step of the reaction with the relative diffusion of binding partners controlling the kinetics of association.

The rates of diffusive encounter of molecules that are measured experimentally can be also predicted theoretically using, for example, Brownian dynamics (BD) simulations,[1−3] a computer simulation technique that is commonly used to study the association kinetics of macromolecules, proteins, and ligands.[4−7] On the basis of such BD simulations, the association rate constant, k, is evaluated as[1−3]

$$k = k_D(b)\frac{\beta}{1-(1-\beta)\frac{k_D(b)}{k_D(c)}} \quad (1)$$

where $k_D(x)$ is the steady-state rate constant of diffusional encounter for two particles with the reaction distance x (where x equals either c or b, and $c > b$) as described in Smoluchowski's theory:[8,9]

$$k_D(x) = 4\pi D(x)x \quad (2)$$

with $D(x)$ being the relative translational diffusion coefficient. Smoluchowski's result was further generalized by Kramers[10] and Debye[11] to account for the forces between particles that may be derived from potentials. The value of $k_D(x)$ can be computed analytically;[12,13] the factor β is the fraction of encounter trajectories, that is, the trajectories that satisfy the predefined reaction criteria, estimated on the basis of BD simulations in which thousands of independent trajectories of the two binding partners are generated.[1−3]

While the direct intermolecular interactions (i.e., electrostatics, polar and nonpolar solvation effects, van der Waals potentials) between diffusing particles in BD simulations are often described with a high level of sophistication,[14,15] the intermolecular hydrodynamic interactions (HIs), resulting from the fact that the moving solute causes movements of the surrounding solvent and that, in turn, the moving solvent displaces other solute molecules, are usually neglected. The reason is either the computational cost of evaluating HIs for coarse-grained bead models of molecular systems[16−18] or the lack of an appropriate (and computationally efficient) theoretical description of HIs for rigid-body BD simulations of arbitrarily shaped molecules.[19]

Only a few attempts to examine the effects of HIs on the kinetics of molecular association have been made so far, either theoretically or through BD simulations.[16,20−27]

Friedman[20] estimated analytically that the hydrodynamic effect reduces about 15% the computed rate constant both for

Received: February 8, 2012
Revised: April 3, 2012
Published: April 18, 2012

   dx.doi.org/10.1021/jp301265y | J. Phys. Chem. B 2012, 116, 5437−5447

neutral species and for ions in aqueous solution. He used the Smoluchowski method that relates the rate of association of spherical particles to the flow in the stationary state, which results after inserting a sink of a radius (i.e., a collision parameter equal or greater to the sum of particle's radii) in an infinite solution of particles with translational diffusion coefficients equal to the relative translational diffusion coefficient of reacting particles.

Larger reduction was predicted on the basis of the approximate solution of the Fokker−Planck equation by Deutch and Felderhof,[21] 46% for association of hard spheres and between 25% and 60% for association of ionic species, depending on the extent of repulsion or attraction between particles.

Wolynes and Deutch[22] showed that when slip boundary conditions are applied instead of stick boundary conditions (that were used in the work of Deutch and Felderhof[21]), the reduction for neutral particles is somewhat smaller, 29% relative to the classical Smoluchowski's theory without HIs. Brune and Kim investigated the hydrodynamic torques occurring when molecules in solution move toward each other and compared their magnitude with the magnitudes of electrostatic torques.[23] Using simple models, these authors demonstrated that the hydrodynamic steering torque can be even 2 orders of magnitude greater than the electrostatic one.

Allison[27] pointed out that mobile ions, which are typically included in the evaluation of electrostatic interactions between the binding partners via screened potentials, should be also considered in the evaluation of hydrodynamic interactions. This concept originates from the work of Hückel, who investigated the influence of ions on the flow of fluid around a charged sphere.[28] Allison proposed a form of the diffusion tensor, *E-tensor*, that accounts for the disturbance of fluid flow by the ions around one of the binding partners when they interact with the other one, and that reduces to the Oseen tensor in the limit of zero salt.[27] Allison analytically computed the association rates of an electron-transfer reaction at different concentrations of salt, modeling HIs with the Oseen tensor with either stick or slip boundary conditions, and with the *E-tensor*. He demonstrated that the latter significantly improves the agreement with experimental results.

Apart from the briefly described theoretical/analytical approaches, there are also studies that investigate the role of HIs in bimolecular association by means of direct BD simulations.[16,24,25] Antosiewicz, Briggs, and McCammon[24,25] investigated the electrostatic and hydrodynamic orientational steering in model enzyme-ligand/substrate systems under various ionic strengths; they obtained an overall decrease of the association rate caused by the hydrodynamic effects in the range of 15−20%. They also concluded that the hydrodynamic complementarity of molecular shapes is most effective at physiological ionic strengths. Fremgen-Kesner and Elcock[16] investigated more elaborate systems, barnase and barstar and their mutants, using coarse-grained Gõ-like models of these proteins (33 pseudoatoms for barnase and 27 pseudoatoms for barstar[16]). They performed BD simulations either with or without intermolecular HIs under various ionic strengths. These authors observed that simulations with HIs turned on yield association rates that are lower up to 80% relative to those obtained from BD simulations without intermolecular HIs. They also observed that the effects of intermolecular HIs are more pronounced when electrostatic interactions between molecules are weakened.[16]

The BD studies described above[16,24,25] use a well-established protocol for simulations of the association processes in systems containing two binding partners in an infinite solvent,[1−3] that along with eqs 1 and 2 allows one to estimate the rates of diffusion-controlled reactions. Their only modification is the inclusion of HIs between binding partners modeled by means of appropriate translational diffusion tensors[29,30] (see also the Methods). However, we note that Fremgen-Kesner and Elcock[16] did not consider that $D(x)$ in eq 2, and thus $k_D(x)$ in eq 1 should be modified to account for HIs between particles,[20] which would affect to some extent their predictions regarding the overall influence of HIs on association kinetics.

In the present work, we investigated the effects of intermolecular hydrodynamic interactions on the kinetics of bimolecular association using the BD technique. As in the above cited studies,[16,20−22,24−27] we consider only the far-field hydrodynamic interactions that are conventionally described at the two-body level. Nevertheless, our approach is different from the ones previously described in refs 16,24,25 in the following ways. First, we studied the association in systems containing model molecules (spheres and dumbbells) with periodic boundary conditions and finite concentrations of reacting species. Second, we describe the association kinetics by means of characteristic association times (waiting times) and rates derived on the basis of the frequency of encounters. Third, we used two different BD algorithms. The simulations with intermolecular HI were performed using the Ermak−McCammon algorithm[17] with HIs modeled with the Ewald-summed form of the translational diffusion tensor appropriate for periodic systems.[31] The simulations without HIs were conducted in the framework of the rigid-body BD algorithm.[32] However, the molecular models used in both kinds of simulations are equivalent. Direct electrostatic and excluded volume interactions between diffusing molecules were taken into account. The simulations were performed at different ionic strengths for charged particles and neutral species, using different definitions of an encounter complex. We analyzed the overall effect of HIs on the kinetics of association and their influence on the relative orientations of binding partners upon diffusive encounters, as well as the interplay between hydrodynamic, electrostatic, and excluded volume interactions.

METHODS

Brownian Dynamics. *Brownian Dynamics of Arbitrarily Shaped Rigid Bodies.* The BD propagation scheme for a number of rigid bodies, described either on a full-atom level or using coarse-grained models, can be written in molecule-fixed frames as:[17,32]

$$\vec{x} = \vec{x}_i^{\,0} + \frac{\Delta t}{k_B T} D_i \vec{M}_i + \vec{R}_i(\Delta t) \tag{3}$$

where i runs over molecules, Δt is the time step, and $\vec{x}$ is the vector describing the position of the center of diffusion[33] $(\vec{r})$ and orientation $(\vec{\phi})$ of the ith molecule, $\vec{x} = (\vec{r},\vec{\phi})^T$. $\vec{M}$ is a generalized force acting on a given particle, having two components: the force acting on the diffusion center $(\vec{F})$, and the torque $(\vec{T})$, where $\vec{M} = (\vec{F},\vec{T})^T$ is evaluated relative to the diffusion center. $\vec{R}(\Delta t)$ is a random displacement vector resulting from the Brownian noise, with zero mean and the variance−covariance given with:

$$\left\langle \vec{R}_i(\Delta t)\vec{R}_j(\Delta t) \right\rangle = 2D_i\delta_{ij}\Delta t \tag{4}$$

dx.doi.org/10.1021/jp301265y | J. Phys. Chem. B 2012, 116, 5437−5447

Here, D is the precomputed, 6 × 6 diffusion tensor of the ith molecule at the diffusion center, containing 3 × 3 blocks related to the translational (tt) and rotational diffusivities (rr) and their couplings (rt,tr):[32]

$$D = \begin{pmatrix} D^{tt} & D^{tr} \\ D^{rt} & D^{rr} \end{pmatrix} \quad (5)$$

Random displacements of particles can be computed via Cholesky decomposition of D.[17] The approach to model Brownian motions of rigid bodies described above neglects interparticle HIs.

Brownian Dynamics with Hydrodynamic Interactions. When HIs are considered during BD simulations, the translational diffusion tensor of the entire system ($3N \times 3N$, with N being the number of spherical molecules or spherical subunits in the so-called bead models of molecules) is used to propagate particles. This tensor depends on the system's configuration and varies with time. The BD propagation scheme can be written as:[17,34]

$$\vec{x} = \vec{x}^{\circ} + \frac{\Delta t}{k_B T} D\vec{F} + \vec{R}(\Delta t) \quad (6)$$

Here, $\vec{F}$ is the $3N$-dimensional vector of forces acting on the centers of spheres; the $3N$-dimensional random displacement vector has zero mean and fulfills $\langle \vec{R}(\Delta t)\vec{R}(\Delta t)\rangle = 2D\Delta t$. Again, random displacements of particles can be computed via Cholesky decomposition of D.[17] However, the decomposition of D (an operation of a computational complexity of $O(N^3)$) must be performed at each BD step due to the dependence of D on the positions of particles.

In the above Ermak–McCammon algorithm[17] (eq 6), hydrodynamic interactions between all spherical particles/subunits can be included by using Oseen[35] or Rotne–Prager–Yamakawa[29,30] forms of the diffusion tensor. For spherical particles with nonequal radii, the latter can be extended as proposed by de la Torre and Bloomfield.[36] As elements of the diffusion tensor correspond to pairwise HIs between all spherical particles in the system and some of these particles can be organized in molecules via appropriate potentials (that correspond to bonds, planar angles, etc.), this approach introduces both intra- and intermolecular HIs. Here, we used the form of the diffusion tensor applicable for nonoverlapping spherical subunits[36] with diagonal and off-diagonal terms defined, respectively, as:

$$D_{ii} = \frac{k_B T}{6\pi\eta a_i}$$

$$D_{ij} = \frac{k_B T}{8\pi\eta r_{ij}}\left(I + \frac{\vec{r}_{ij}\vec{r}_{ij}^{\,T}}{r_{ij}^2} + \frac{a_i^2 + a_j^2}{r_{ij}^2}\left(\frac{1}{3}I - \frac{\vec{r}_{ij}\vec{r}_{ij}^{\,T}}{r_{ij}^2}\right)\right) \quad (7)$$

where η is the viscosity of the solvent, r_{ij} is the distance between spheres i and j (of hydrodynamic radii a_i and a_j), and I is the unit tensor. BD simulations were performed for finite simulation boxes containing molecules, and diffusion tensors were evaluated using the Ewald summation technique, as described elsewhere[31] (implementation details can be found in ref 18); this approach prevents the diffusion tensor from becoming nonpositive definite, which is a condition that has to be met to use diffusion tensors as covariance matrices.[31] At each BD simulation step, the Ewald-summed diffusion tensor of the whole simulated system is factorized using the Cholesky decomposition[17] to obtain hydrodynamically correlated displacements of particles.

Direct Interparticle Interactions. Electrostatic interactions are modeled using the Debye–Hückel approximation.[37] Within this approach, spherical particles (of radii a_i, a_j) with central net charges (q_i, q_j) interact via pairwise-additive potentials:

$$V(r_{ij}) = \frac{q_i q_j}{4\pi\varepsilon_0\varepsilon(1 + \kappa a_i)(1 + \kappa a_j) r_{ij}} e^{-\kappa(r_{ij} - a_i - a_j)} \quad (8)$$

where ε_o is the vacuum permittivity, ε is the dielectric constant of the solvent, κ is the inverse of the Debye screening length,[37] and r_{ij} is the separation between particles. Electrostatic forces computed as a gradient of the above expression are evaluated within spherical cutoffs.

Excluded volume interactions are modeled with the standard attractive/repulsive, 6/12 Lennard-Jones potential:

$$V(r_{ij}) = 4\varepsilon_{LJ}\left(\left(\frac{a_i + a_j}{r_{ij}}\right)^{12} - \left(\frac{a_i + a_j}{r_{ij}}\right)^{6}\right) \quad (9)$$

where ε_{LJ} is the potential well depth. However, in our simulations, a cutoff of $2^{1/6}(a_i + a_j)$ was applied during evaluation of Lennard-Jones interactions, and effectively only the short-range repulsion between particles was taken into account.

Brownian Dynamics Simulations. *Model Systems.* Because our aim was to study the process of electrostatically driven association, we used the systems containing particles with opposite total net charges. The diffusional encounters were investigated in the following two model systems. The first system consisted of two oppositely charged (+10e and −10e) spherical particles of identical radii of 15 Å. The second system contained two oppositely charged dumbbells, each consisting of two nonoverlapping spheres of 15 Å radii, separated by 32 Å, with +10e and −10e charges at their centers (Figure 1).

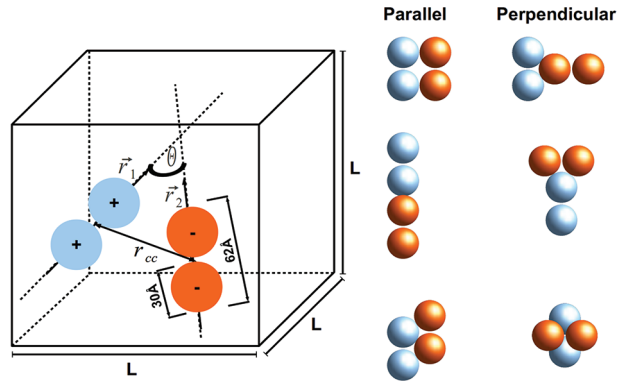

Figure 1. The scheme of the simulation setup and parameters that were used to define the reaction criteria. Examples of parallel and perpendicular encounter complexes are also shown. See text for details.

Additionally, the systems of dumbbells and spheres with zeroed partial charges were considered; we will further refer to them using the term "neutral". Each system was simulated either with the rigid-body BD algorithm (without intermolecular HIs) or with the Ermak–McCammon algorithm (with intermolecular HIs included). In the latter, spherical subunits of dumbbells

dx.doi.org/10.1021/jp301265y | J. Phys. Chem. B 2012, 116, 5437–5447

were connected with an elastic bond of an equilibrium value of 32 Å.

For isotropic, spherical molecules, comparing the results of BD simulations performed with both algorithms is straightforward because the translational part of the sphere's rigid-body diffusion tensor consists simply of its identical diffusion coefficients in three directions, $D_i^{tt} = D_{ii} = (k_B T)/(6\pi\eta a_i)$ (see eqs 5 and 6), and all $D^{rt,tr}$ are zero due to the uncoupling of rotations and translations. Moreover, rotations of spheres are irrelevant because we treat them as uniformly reactive.

However, the situation gets more complicated in case of dumbbell particles. While with the rigid-body BD algorithm the rotations of a dumbbell are modeled explicitly, in the Ermak–McCammon algorithm only translational motions of dumbbells' subunits are considered, and correct rotations of a dumbbell as a whole arise from their hydrodynamically correlated motions.[34] To compare the results of both kinds of simulations directly, we need to use the models of particles that are hydrodynamically equivalent. For that, we performed the computations described below.

First, we evaluated the rigid-body diffusion tensor of a dumbbell using rigid-body hydrodynamic calculations, with the program developed by one of the authors of this work.[38] Next, we performed multiple BD simulations of a single dumbbell with both algorithms and analyzed its translations. Precisely, we examined the mean square displacement of the center of diffusion, which in this case is also the geometric center of a dumbbell (Figure 2). Both algorithms gave the same diffusional

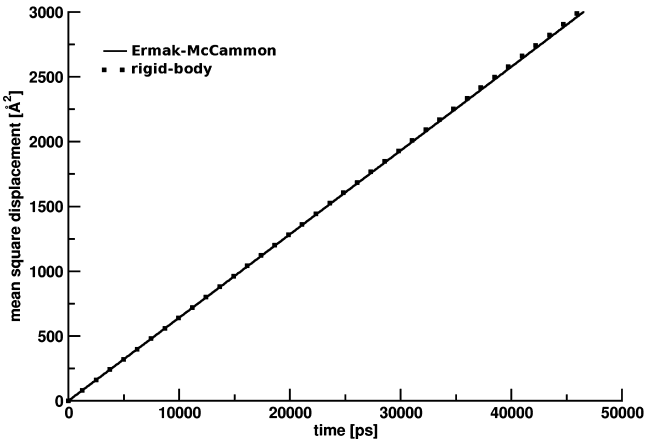

Figure 2. Mean square displacement of a single dumbbell derived from BD trajectories. BD simulations were either with the rigid-body BD algorithm[32] or with the Ermak–McCammon algorithm,[17] and the dumbbell was modeled as two beads connected with a harmonic bond.

translational behavior that was also in agreement with rigid-body hydrodynamic calculations.

Next, we examined rotational diffusion, which in case of a dumbbell is not hydrodynamically coupled to translations and can be examined separately. We analyzed the rotational correlation function:

$$C(t) = \langle P_2(\vec{u}(t)) P_2(\vec{u}(t + \Delta t)) \rangle \quad (10)$$

with $P_2(x) = (1/2)(3x^2 - 1)$ denoting the second Legendre polynomial[32] of a unit vector $(\vec{u})$ pointing along the line connecting the centers of dumbbell's spherical subunits. As described in refs 39–41 for an isolated object, this correlation function is determined solely by the eigenvalues of the rotational diffusion tensor, D^{rr}, and the orientation of the vector $\vec{u}$ rigidly attached to the rotating object. To obtain agreement between the results of both kinds of simulations (Figure 3), which in turn assures that both dumbbell models

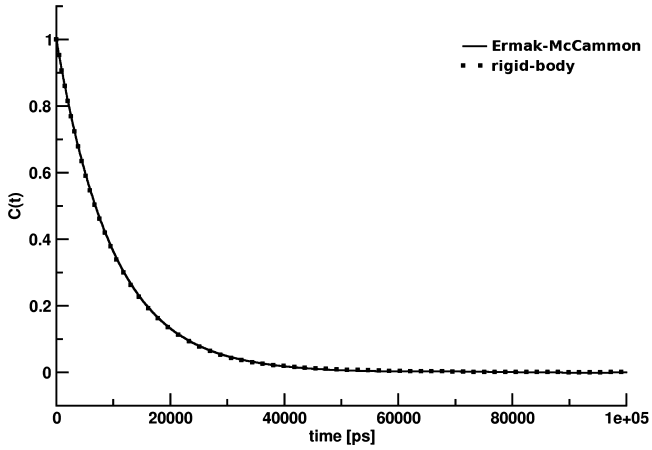

Figure 3. Rotational correlation functions derived from BD trajectories of a single dumbbell simulated either with the rigid-body BD algorithm[32] or as two beads connected with a harmonic bond with the Ermak–McCammon algorithm.[17]

are equivalent considering their rotational diffusion, we adjusted these values of the D^{rr} block in the dumbbell's rigid-body diffusion tensor that correspond to the rotations around the axes perpendicular to the direction of $\vec{u}$. In the studied case, these values are equal and can be deduced directly from $\langle P_2(\vec{u}(t)) P_2(\vec{u}(t + \Delta t)) \rangle$.[39−41] The rotation around the axis parallel to $\vec{u}$ is not relevant in this case due to the symmetry of a dumbbell. Also, note that the rotation of a dumbbell around this axis cannot be accounted for within the framework of the Ermak–McCammon algorithm. The reason for the initially observed discrepancy between the results of rigid-body hydrodynamic calculations (which are of course the same as those of rigid-body BD simulations) and BD simulations with the Ermak–McCammon algorithm is the presence of the elastic bond between the subunits. This elastic bond allows for small fluctuations in the mutual distance of the subunits, which affects the HIs between them and thus the overall rotations of a dumbbell.

Simulation Setup. All BD simulations were performed using a primary simulation cell of size 225 Å × 225 Å × 225 Å. This cell contains either two oppositely charged spheres or two oppositely charged dumbbells. Such a choice of the primary simulation cell size was dictated by the need of gathering sufficient statistics of the particle encounters, and increasing the cell size decreases the number of encounters observed during a particular time interval. Additionally, with such a choice of cell size, the simulated systems can be still treated as dilute with the two dumbbells (spheres) occupying roughly 0.5% (0.25%) of the cell's volume. For the simulations with the Ermak–McCammon algorithm, HIs were evaluated using the direct Ewald summation procedure[18] over a three-dimensional matrix containing 125 copies of the primary cell, which assured the convergence of the sum.

The simulations were carried out at ionic strengths of 0.1, 0.15, 0.2, 0.25, 0.3, and 0.5 M. Electrostatic interactions were evaluated within a spherical cutoff of 100 Å. Additionally, simulations of uncharged systems were also performed. The

dx.doi.org/10.1021/jp301265y | J. Phys. Chem. B 2012, 116, 5437−5447

well depth of Lennard-Jones interactions (ε_{LJ} in eq 9) was set to 0.5922 kcal/mol. Apart from the short-range Lennard-Jones repulsion, we prevent (similarly in both kinds of simulations) from eventual overlaps between particles by revoking and subsequently repeating (with a new vector of random displacements) each step of a BD simulation that leads to an overlap. A similar procedure was used previously in the studies of limited diffusion in the presence of infinite planes[32] and simulations of multicomponent protein systems.[42,43]

Simulations were performed at the temperature of 298.15 K with water viscosity set to 0.01 poise. For each ionic strength and for neutral systems, we generated 5000 BD trajectories with both algorithms. Each trajectory started with molecules placed at random positions and orientations inside the primary simulation cell. The time step used in both algorithms was 4 ps. Duration of a single trajectory was thus 4 μs, totaling to 20 *ms* per each considered ionic strength and neutral systems. Snapshots from trajectories were recorded every 100 ps.

Simulations with enabled intermolecular HIs were performed using the BD_BOX package.[18] Rigid-body BD simulations were performed with an in-house software.

Trajectory Analysis. *Association (Waiting) Times.* From each of the generated BD trajectories we extracted the center-to-center distance between diffusing objects (r_{cc}) and the angle θ between the vectors rigidly attached to the objects (see Figure 1) as functions of time. We took into account the periodic images of objects, so r_{cc} and θ (in case of dumbbells) were measured for either a pair of objects in the primary simulation box or an object in the primary simulation box and the nearest periodic image of the second object. The r_{cc} and θ parameters (Figure 1) effectively constitute a reaction coordinate (Figure 4) that was used to monitor the progress of association.

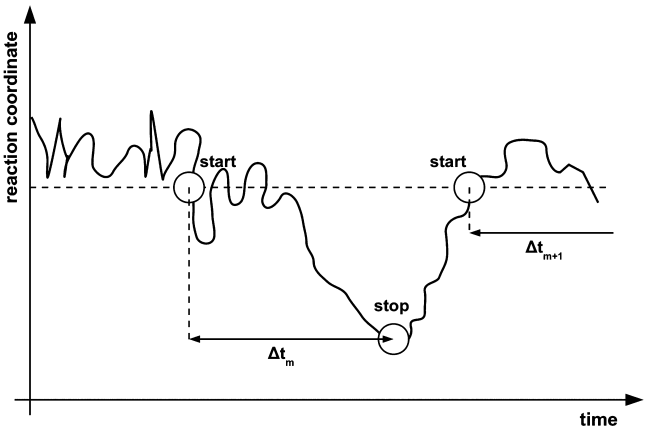

Figure 4. Progress of a reaction coordinate (r_{cc}, θ) over a simulation time during a BD trajectory. The "start" and "stop" points correspond to the fully dissociated binding partners and their complex (defined for a particular distance r_{cc} and angle θ), respectively. The durations, Δt, were stored for various definitions of the reaction criteria and next used to describe association kinetics as described in the text.

From each BD trajectory generated for particular conditions (such as ionic strength, the presence or absence of HIs), we extracted the time courses of the reaction coordinate. Next, we measured the durations of continuous fragments of these times that begin when the reaction coordinate reaches the "start" value (objects are dissociated) and end when the reaction coordinate reaches the "stop" value (objects form a complex according to the predefined reaction criteria). For a scheme, see Figure 4. Next, the average duration was computed resulting in the average association time, which can be also treated as the average waiting time for a diffusional encounter.

Rate Constants. The reaction rate constants were computed assuming irreversible association of particles using:

$$k = \frac{n_{react}}{\Delta T \cdot N_A \cdot V \cdot [A]^2} \tag{11}$$

where n_{react} is the number of encounters observed during time ΔT, N_A is the Avogadro number, V is the volume of the simulation cell, and [A] is the concentration of either one of the diffusing species. The k values from different trajectories were averaged resulting in the mean values of association rate constants.

RESULTS

Equilibrium Properties of Dumbbell Systems. Reaction Criteria. To investigate the equilibrium properties of dumbbells, we constructed plots of the average of the second Legendre polynomial of the cosine of the θ angle (Figure 1), $P_2(\cos\theta)$, as a function of the dumbbells' center-to-center distance, r_{cc}, for different simulation conditions. These plots are shown in Figure 5. The plots obtained with the rigid-body and the Ermak−McCammon BD algorithms under various conditions are similar because HIs do not modify the equilibrium properties of this system. The similarity of these

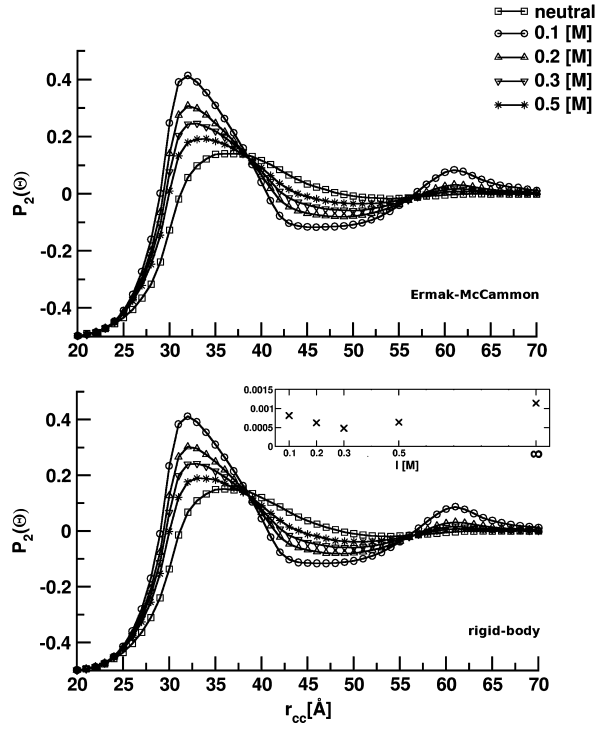

Figure 5. The average of the second Legendre polynomial for the cos θ as a function of the interparticle separation r_{cc} derived from BD simulations with HIs (with the Ermak−McCammon algorithm, top) and from rigid-body BD simulations (bottom) conducted for neutral and charged dumbbells at different ionic strengths. Inset: Residual sum of squares $(\sum_{rcc}(P_2^{HI}(\theta;r_{cc}) - P_2^{rigid}(\theta;r_{cc}))^2$ where "HI" denotes the Ermak−McCammon algorithm and "rigid" the rigid-body algorithm) obtained after comparing corresponding plots generated at different ionic strengths; the symbol ∞ corresponds to the system of neutral dumbbells.

dx.doi.org/10.1021/jp301265y | J. Phys. Chem. B 2012, 116, 5437−5447

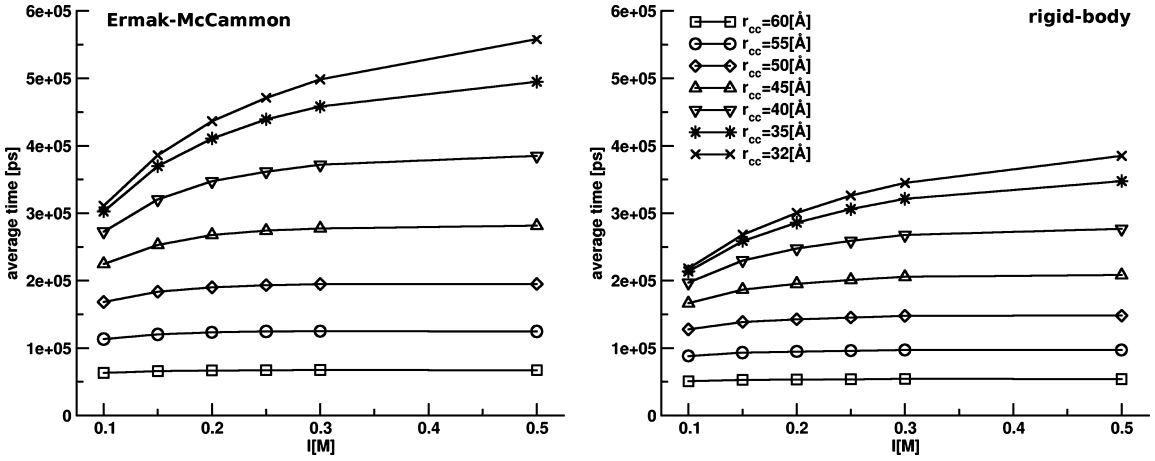

Figure 6. Average association times obtained for spherical molecules for different reaction criteria (r_{cc} distance) as a function of ionic strength. Left: Simulations with the Ermak−McCammon algorithm with interparticle HIs. Right: Rigid-body BD simulations without interparticle HIs.

plots is an additional confirmation (together with the mean square displacements data and rotational correlation functions presented above) that both approaches used in this work to model dumbbells (rigid-body and the beads and spring models) are indeed equivalent.

For large intermolecular separations of 70 Å and above, the average $P_2(\cos\theta)$ approaches zero in all cases, that is, for the simulations of neutral molecules and charged molecules at different ionic strengths (Figure 5). This indicates that at equilibrium there are no preferences regarding the relative orientations of molecules separated by such a distance. However, as molecules get closer and r_{cc} decreases, the plots of average $P_2(\cos\theta)$ show extrema at different r_{cc}. These extrema result from the electrostatic and excluded volume interactions between dumbbells.

For neutral particles, there is a wide maximum in $P_2(\cos\theta)$ around r_{cc} of 35 Å that corresponds to a combination of parallel (as $P_2(\cos(0)) = 1$ and $P_2(\cos(\pi)) = 1$) and perpendicular (as $P_2(\cos(\pi/2)) = -0.5$) orientations of particles; these are the preferred orientations considering the short-range Lennard-Jones repulsion between the dumbbells' spherical subunits and steric hindrance. For center-to-center distances smaller than 35 Å, the perpendicular relative orientations of particles start to prevail due to steric hindrance; at r_{cc} of about 20 Å, $P_2(\cos\theta)$ reaches its minimum of −0.5 (Figure 5).

Introducing electrostatic interactions results in additional extrema on the plots of average $P_2(\cos\theta)$. Apart from the maximum around 35 Å, we note that electrostatic interactions stabilize the parallel orientations at r_{cc} equal to about 62 Å (which is the distance between the centers of dumbbells in the head-to-head or head-to-tail configuration, i.e., when the two dumbbells are aligned; see also Figure 1). Below 60 Å, when excluded volume interactions between dumbbells come into play, there is a wide minimum signifying an additional stabilization of perpendicular relative orientations. These orientational preferences are more pronounced when electrostatic interactions become stronger because the observed extrema become narrower and higher/deeper when the ionic strength is lower.

On the basis of the above analyses, we studied the kinetics of specific and nonspecific association of dumbbells. By specific association, we mean the formation of complexes in which the relative orientations of binding partners are either parallel or perpendicular for various r_{cc} distances. Because one of the binding partners consists of two spherical subunits that bear central positive charges and the other one of subunits that bear negative charges, both orientations are energetically stable from the electrostatic standpoint. By nonspecific association, we denote the formation of complexes that satisfy the reaction criteria defined only based on the center-to-center distance of binding partners, regardless of their orientations. Additionally, for association of dumbbells, we define the outer boundary of the encounter complex (the "start" parameter in Figure 4) when r_{cc} is equal to 70 Å. The binding partners are considered to be fully dissociated when their center-to-center separation is greater than 70 Å.

Nonspecific Association of Spherical Particles. The first system considered by us to study an overall effect of HIs on association kinetics consisted of two spherical particles, either neutral or bearing central charges of the same magnitude but opposite signs. We analyzed the association times (see the Methods) using the center-to-center distance (r_{cc}) of spheres as a single reaction criterion. The dissociated state of reactants ("start" in Figure 4) was assumed for r_{cc} equal to 65 Å (whereas the sum of spheres' radii is 30 Å). The average association times derived from simulations of charged particles at different ionic strengths, either with or without HIs, are given in Figure 6. Generally, the introduction of interparticle HIs leads to longer association times (Figure 6) and as a consequence to smaller association rates. Moreover, the ratio T^{HI}/T^{rigid} (with T^{HI} being the average association time derived from simulations with HIs, and T^{rigid} the average association time from rigid-body BD simulations that do not take into account hydrodynamic interactions between associating molecules) does not depend on the ionic strength, but only on r_{cc} of the encounter complex (see Table 1). As HIs are proportional to the inverse of the distance between diffusing spheres (eq 6), this ratio increases from 1.246 ± 0.004 to almost 1.44 ± 0.01 (averages are over the values derived from BD simulations conducted at different ionic strengths) upon decreasing r_{cc} from 60 to 32 Å, regardless of the value of the ionic strength. Similar values of T^{HI}/T^{rigid} were obtained from BD simulations with neutral particles. Therefore, one can conclude that for spherical, uniformly reactive particles, the contribution to the association kinetics of interparticle HIs remains the same regardless of the presence or absence of direct interparticle interactions and their strength, at least in the framework of the hydrodynamic model considered in this work.

dx.doi.org/10.1021/jp301265y | J. Phys. Chem. B 2012, 116, 5437−5447

Table 1. Ratios T^{HI}/T^{rigid} Derived for Spheres and Dumbbell Particles from BD Simulations at Different Ionic strengths and for Neutral Particles (∞)[a]

	T^{HI}/T^{rigid} (spheres)			T^{HI}/T^{rigid} (dumbbells)
I [M]	r_{cc} = 60 Å	r_{cc} = 45 Å	r_{cc} = 35 Å	r_{cc} = 65 Å
0.1	1.243	1.349	1.416	1.460
0.15	1.245	1.355	1.428	1.454
0.2	1.252	1.370	1.436	1.447
0.25	1.251	1.363	1.436	1.435
0.3	1.243	1.349	1.426	1.474
0.5	1.243	1.352	1.424	1.437
∞	1.246	1.358	1.419	1.446

[a]Results are for non-specific association.

Association of Anisotropic Particles. *Nonspecific Association.* We conducted analysis similar to the one described above for a system of dumbbell molecules. We analyzed association times derived from BD simulations for r_{cc} in the encounter complex set to 65 Å (for such a value of dumbbells' center-to-center distance, excluded volume interactions play no role upon their encounter) and without any restrictions regarding relative orientations of the binding partners in the complex. The results obtained for such a definition of the encounter complex are shown in Figure 7.

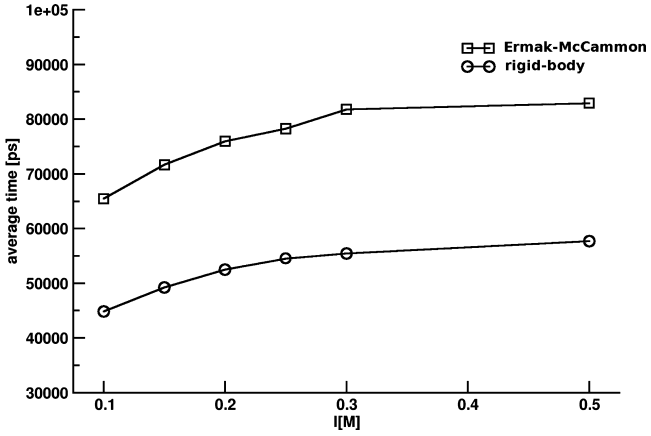

Figure 7. Average association times obtained for charged dumbbell particles at different ionic strengths either with (the Ermak–McCammon algorithm) or without (the rigid-body algorithm) interparticle HIs when the only reaction criterion is the center-to-center distance of particles (r_{cc}). Results for r_{cc} = 65 Å.

Similarly as for uniformly reactive spheres, HIs cause longer association times and slower association. Interestingly, for dumbbells we also obtained almost similar ratios T^{HI}/T^{rigid} for different ionic strengths and for neutral molecules (see Table 1). Averaging the values obtained from simulations at different ionic strengths and for neutral particles gives 1.45 ± 0.01. We thus conclude that the relative magnitude of the HI effects on the kinetics of association does not depend on the strength of direct interparticle interactions even though particles are anisotropic considering both their hydrodynamic and their electrostatic properties.

Specific Association. Figure 8 shows the average association times derived from BD simulations of dumbbells for different definitions of the encounter complex that apart from the r_{cc} distance include also relative orientations of particles (either parallel or perpendicular). Again, we observe that the overall

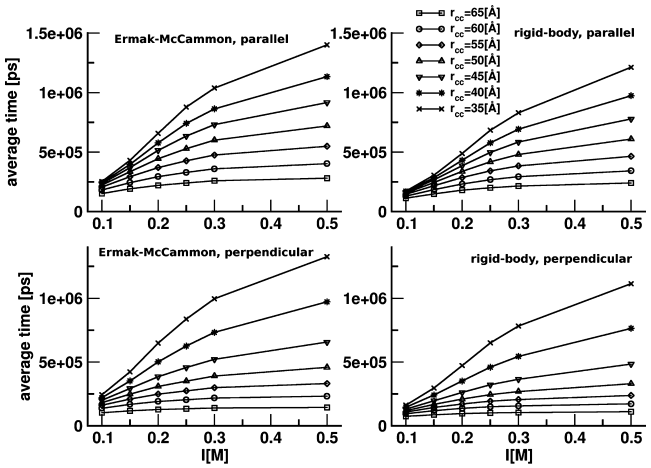

Figure 8. Average association times obtained for charged dumbbell particles at different ionic strengths from BD simulations either with (the Ermak–McCammon algorithm) or without (the rigid-body algorithm) interparticle HIs, for different center-to-center distances (r_{cc}) and orientations (parallel/perpendicular) in an encounter complex.

effect of introducing HIs is to increase association times and to slow association kinetics.

However, when the orientation of the binding partners is incorporated into the definition of the encounter complex (parallel or perpendicular complexes), the situation is quite different than the one observed for association of nonspecific dumbbells. For example, for r_{cc} = 65 Å, the ratio T^{HI}/T^{rigid} is about 1.35 at I = 0.1 M, 1.20 at I = 0.3 M, 1.15 at I = 0.5 M, and 1.15 for neutral dumbbells in case of the parallel encounter. For perpendicular encounters, the corresponding values are 1.40, 1.35, 1.30, and 1.30. The HI effects are thus no longer independent of the strength of electrostatic interactions. Moreover, for particular reaction criteria (i.e., either parallel or perpendicular), their relative magnitude increases with an increasing strength of electrostatic interactions. The smallest contributions arising from HIs are observed for neutral particles. These results lead to the conclusion that there is an interplay between the ionic screening and HIs affecting the relative orientations of diffusing molecules. Interestingly, for nonspecific association and r_{cc} of 65 Å, the ratio T^{HI}/T^{rigid} at 0.1 M ionic strength is 1.45 ± 0.01, larger than the values obtained for both parallel and perpendicular encounters. Additionally, when r_{cc} in the encounter complex is decreased to 35 Å, the ratio T^{HI}/T^{rigid} is about 1.45 at I = 0.1 M, 1.25 at I = 0.3 M, 1.15 at I = 0.5 M, and 1.05 for neutral dumbbells in case of a parallel encounter. For perpendicular encounters, we obtain ratios of 1.50, 1.27, 1.20, and 1.10, respectively. The magnitude of the HI effects is more affected upon changing the strength of electrostatic interactions both for parallel and for perpendicular encounters than in case of r_{cc} = 65 Å. Additionally, the T^{HI}/T^{rigid} ratios for parallel and perpendicular encounters obtained at particular ionic strengths and for neutral systems converge toward each other, which is a consequence of the excluded volume interactions that impede the relative diffusion of the binding partners at small separations.

Association Rate Constants. In case of associating dumbbell particles, we computed the absolute association rate constants as described in the Methods, for different definitions of the encounter complex and for different BD simulations. Their values are given in Table 2. Overall, the association toward the

dx.doi.org/10.1021/jp301265y | J. Phys. Chem. B 2012, 116, 5437–5447

Table 2. Association Rates Derived for Dumbbell Particles from BD Simulations Either with (HI) or without (Rigid) Interparticle HIs, for Different Definitions of the Encounter Complex, r_{cc}, and for Either Parallel (∥) or Perpendicular (⊥) Relative Orientations of the Binding Partners[a]

I [M]	$k_{\parallel}^{HI}$ [1/Ms]	$k_{\parallel}^{rigid}$ [1/Ms]	$k_{\perp}^{HI}$ [1/Ms]	$k_{\perp}^{rigid}$ [1/Ms]
		r_{cc} = 65 Å		
0.1	(6.52 ± 0.08) × 10^{10}	(7.43 ± 0.07) × 10^{10}	(1.05 ± 0.01) × 10^{11}	(1.22 ± 0.01) × 10^{11}
0.15	(3.83 ± 0.03) × 10^{10}	(4.75 ± 0.03) × 10^{10}	(6.28 ± 0.04) × 10^{10}	(8.23 ± 0.04) × 10^{10}
0.2	(3.20 ± 0.02) × 10^{10}	(3.87 ± 0.02) × 10^{10}	(5.52 ± 0.03) × 10^{10}	(7.29 ± 0.04) × 10^{10}
0.25	(2.92 ± 0.02) × 10^{10}	(3.44 ± 0.02) × 10^{10}	(5.23 ± 0.03) × 10^{10}	(6.84 ± 0.03) × 10^{10}
0.3	(2.71 ± 0.03) × 10^{10}	(3.22 ± 0.02) × 10^{10}	(4.95 ± 0.03) × 10^{10}	(6.60 ± 0.03) × 10^{10}
0.5	(2.47 ± 0.02) × 10^{10}	(2.85 ± 0.02) × 10^{10}	(4.78 ± 0.03) × 10^{10}	(6.17 ± 0.03) × 10^{10}
∞	(2.31 ± 0.01) × 10^{10}	(2.68 ± 0.02) × 10^{10}	(4.63 ± 0.03) × 10^{10}	(5.99 ± 0.03) × 10^{10}
		r_{cc} = 55 Å		
0.1	(4.73 ± 0.05) × 10^{10}	(5.77 ± 0.05) × 10^{10}	(6.74 ± 0.09) × 10^{10}	(8.46 ± 0.08) × 10^{10}
0.15	(2.53 ± 0.02) × 10^{10}	(3.28 ± 0.02) × 10^{10}	(3.56 ± 0.03) × 10^{10}	(5.00 ± 0.03) × 10^{10}
0.2	(1.94 ± 0.02) × 10^{10}	(2.44 ± 0.01) × 10^{10}	(2.86 ± 0.02) × 10^{10}	(4.09 ± 0.02) × 10^{10}
0.25	(1.67 ± 0.02) × 10^{10}	(2.04 ± 0.01) × 10^{10}	(2.56 ± 0.02) × 10^{10}	(3.59 ± 0.02) × 10^{10}
0.3	(1.53 ± 0.02) × 10^{10}	(1.81 ± 0.01) × 10^{10}	(2.35 ± 0.01) × 10^{10}	(3.35 ± 0.02) × 10^{10}
0.5	(1.32 ± 0.01) × 10^{10}	(1.52 ± 0.01) × 10^{10}	(2.11 ± 0.01) × 10^{10}	(2.89 ± 0.01) × 10^{10}
∞	(1.20 ± 0.02) × 10^{10}	(1.39 ± 0.02) × 10^{10}	(1.94 ± 0.01) × 10^{10}	(2.60 ± 0.01) × 10^{10}
		r_{cc} = 45 Å		
0.1	(4.02 ± 0.04) × 10^{10}	(5.13 ± 0.04) × 10^{10}	(5.19 ± 0.06) × 10^{10}	(6.77 ± 0.06) × 10^{10}
0.15	(2.01 ± 0.02) × 10^{10}	(2.67 ± 0.02) × 10^{10}	(2.55 ± 0.02) × 10^{10}	(3.64 ± 0.02) × 10^{10}
0.2	(1.42 ± 0.01) × 10^{10}	(1.82 ± 0.01) × 10^{10}	(1.86 ± 0.01) × 10^{10}	(2.68 ± 0.01) × 10^{10}
0.25	(1.16 ± 0.01) × 10^{10}	(1.47 ± 0.02) × 10^{10}	(1.57 ± 0.01) × 10^{10}	(2.17 ± 0.01) × 10^{10}
0.3	(1.07 ± 0.02) × 10^{10}	(1.27 ± 0.02) × 10^{10}	(1.41 ± 0.02) × 10^{10}	(1.91 ± 0.01) × 10^{10}
0.5	(0.94 ± 0.02) × 10^{10}	(1.01 ± 0.02) × 10^{10}	(1.14 ± 0.01) × 10^{10}	(1.46 ± 0.01) × 10^{10}
∞	(0.92 ± 0.03) × 10^{10}	(0.96 ± 0.03) × 10^{10}	(0.98 ± 0.02) × 10^{10}	(1.15 ± 0.01) × 10^{10}
		r_{cc} = 35 Å		
0.1	(3.64 ± 0.04) × 10^{10}	(4.78 ± 0.04) × 10^{10}	(3.86 ± 0.04) × 10^{10}	(5.16 ± 0.04) × 10^{10}
0.15	(1.72 ± 0.02) × 10^{10}	(2.33 ± 0.01) × 10^{10}	(1.76 ± 0.02) × 10^{10}	(2.41 ± 0.01) × 10^{10}
0.2	(1.14 ± 0.01) × 10^{10}	(1.46 ± 0.01) × 10^{10}	(1.15 ± 0.01) × 10^{10}	(1.50 ± 0.01) × 10^{10}
0.25	(0.93 ± 0.01) × 10^{10}	(1.11 ± 0.02) × 10^{10}	(0.96 ± 0.01) × 10^{10}	(1.15 ± 0.03) × 10^{10}
0.3	(0.88 ± 0.02) × 10^{10}	(0.99 ± 0.02) × 10^{10}	(0.89 ± 0.02) × 10^{10}	(1.03 ± 0.02) × 10^{10}
0.5	(0.81 ± 0.03) × 10^{10}	(0.89 ± 0.03) × 10^{10}	(0.81 ± 0.02) × 10^{10}	(0.87 ± 0.03) × 10^{10}
∞	(0.88 ± 0.04) × 10^{10}	(0.93 ± 0.06) × 10^{10}	(0.84 ± 0.03) × 10^{10}	(0.93 ± 0.06) × 10^{10}

[a]The ∞ symbol corresponds to BD simulations of neutral particles. Errors represent the standard deviation of the mean.

parallel encounter is slower than that toward the perpendicular encounter. However, as r_{cc} in the encounter complex gets smaller, the differences in the absolute rates of parallel and perpendicular encounters start to diminish. Additionally, both parallel and perpendicular encounters are slowed when the intermolecular HIs are included. The association rate constants derived from all BD simulations monotonically decrease with the increasing ionic strength, regardless of the definition of the encounter complex.

To examine the contributions of interparticle HIs to the kinetics of association, we created the plots of the ratio $k^{rigid} - k^{HI}/k^{rigid}$ (with indices "rigid" and "HI" denoting BD simulations conducted with the rigid-body and Ermak–McCammon BD algorithm, respectively) as a function of ionic strength for a particular reaction criterion and as a function of the reaction criteria for a particular ionic strength. These plots illustrate the balance between hydrodynamic, electrostatic, and excluded volume interactions under different conditions (Figures 9 and 10).

Figure 9 shows the contributions of interparticle HIs to the association rate constants of parallel and perpendicular encounters as a function of ionic strength for different r_{cc} values. For r_{cc} of 65 Å and low ionic strength of 0.1 M, both parallel and perpendicular encounters are slowed by HIs in a comparable manner, by about 10%. However, upon increasing the ionic strength, when electrostatic interactions between the binding partners are weakened, HIs differently contribute to the association kinetics in case of parallel and perpendicular encounters. For parallel encounters, the maximal effect of HIs is observed at ionic strength of 0.15 M, about 20%; then, upon increasing the ionic strength, the effect of HIs monotonically decreases, reaching about 15% at ionic strength of 0.5 M. On the other hand, for perpendicular encounters, the effects of HIs are almost similar for all ionic strengths above 0.15 M, about 25%. As association rates of perpendicular encounters are more affected by HIs than those of parallel ones, we conclude that the parallel encounters are hydrodynamically more favored and HIs rather oppose perpendicular orientations of molecules upon their encounter. Overall, with no significant steric hindrance upon encounter, the differences in the orientational hydrodynamic preferences diminish at low ionic strengths and become more visible at higher ionic strengths.

When electrostatic interactions are magnified by allowing smaller r_{cc} in the encounter complexes, the overall effects of HIs on association rates become more pronounced in both parallel (up to 25%) and perpendicular encounters (up to 30%) at lower ionic strength (below 0.3 M). However, at ionic strengths above 0.3 M, the HI effects are less visible, in case of both

dx.doi.org/10.1021/jp301265y | J. Phys. Chem. B 2012, 116, 5437–5447

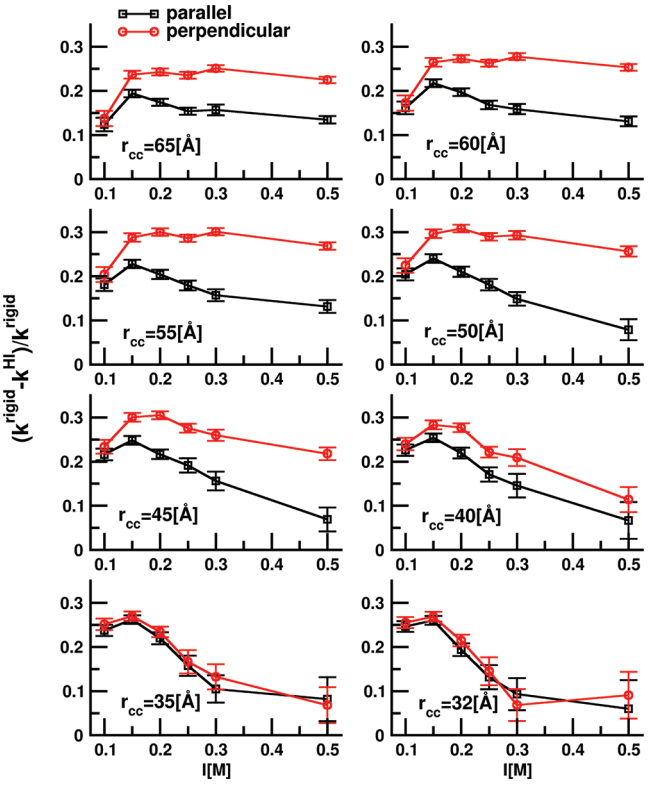

Figure 9. Effects of interparticle HIs on the association rate constants obtained for charged dumbbell particles as a function of ionic strength. The results are shown for different reaction criteria.

parallel and perpendicular encounters. Moreover, for r_{cc} below 40 Å, the hydrodynamic preference for parallel orientations of binding partners vanishes; that is, contributions of HIs to the association rates for parallel and perpendicular encounters are similar at the whole range of considered ionic strengths. We attribute this behavior to both electrostatic interactions, which stabilize both orientations, and excluded volume interactions. Direct intermolecular interactions become more and more prominent with decreasing r_{cc} to finally overcome the influence of HIs on the relative orientation of binding partners.

An additional illustration of the effects of different interactions on the kinetics of diffusional encounters is shown in Figure 10, which contains the plots of the $(k^{rigid} - k^{HI})/k^{rigid}$ ratio as a function of r_{cc} in an encounter complex for different ionic strengths. At low ionic strength of 0.1 M, when electrostatic interactions are strong, the contributions of HIs to association rate constants are similar for parallel and perpendicular encounters in the whole range of r_{cc}. These contributions are largest (about 30%) when r_{cc} is 32 Å and smallest when r_{cc} is set to 65 Å. Therefore, it seems clear that while significant electrostatic interactions magnify the overall effect of HIs on the kinetics of association, they also destroy the hydrodynamic preference for a particular orientation of binding partners upon an encounter. Upon increasing the ionic strength to 0.5 M, we observe that, from the hydrodynamic standpoint, parallel encounters are preferred. This happens because after introducing HIs the rates of parallel encounters are less affected than the rates of perpendicular ones, for r_{cc} larger than 40 Å (Figure 10). However, below this value of r_{cc}, the excluded volume interactions between binding partners additionally impede the hydrodynamic orientational effects. The role of excluded volume interactions in close encounters is also clear when we consider the $(k^{rigid} - k^{HI})/k^{rigid}$ ratios from the BD simulations of neutral dumbbells. For r_{cc} equal to 65 Å, we obtain HIs contributions of nearly 15% for parallel encounters and about 25% for perpendicular encounters. For r_{cc} equal to 35 Å, HIs contributions drop below 10% in both cases.

From Figures 9 and 10 one can also conclude that the largest contributions of interparticle HIs to association rates are observed for moderate, close to physiologic, ionic strengths, which resembles the result obtained by Antosiewicz, Briggs, and McCammon.[24]

DISCUSSION

We performed Brownian dynamics simulations of charged and neutral, isotropic and anisotropic model molecules to examine the contributions of interparticle hydrodynamic interactions to the kinetics of electrostatically driven bimolecular association. Hydrodynamic interactions were modeled via Rotner−Prage−Yamakawa translational diffusion tensors[29,30] evaluated using the Ewald summation procedure, appropriate for the periodic system.

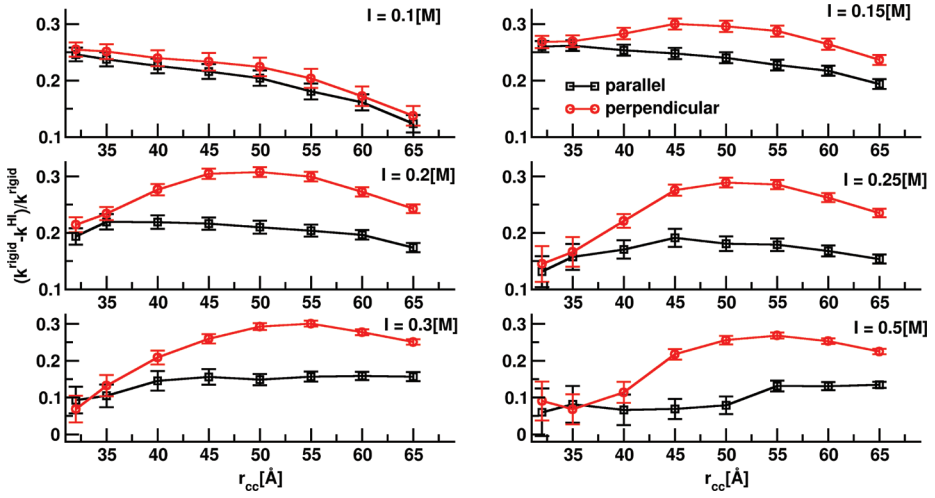

Figure 10. Effects of interparticle HIs on association rate constants obtained for charged dumbbell particles as a function of reaction criteria. The results are shown for various ionic strengths.

dx.doi.org/10.1021/jp301265y | J. Phys. Chem. B 2012, 116, 5437−5447

For a system of spherical particles, either neutral or with charges positioned at their centers, we observe that association is slower when hydrodynamic interactions between particles are taken into account. Generally, this result corroborates with previous theoretical works.[20−22] Moreover, the contributions of HIs to nonspecific association of spherical particles are similar regardless of the particles's charges. Again, the same was observed by Friedman[20] who used an approximate theory. Additionally, in case of spherical particles, we do not observe any dependence of the relative hydrodynamic effect on the ionic strength of the solution. However, a different result was obtained by Deutch and Felderhof,[21] who, based on the analytical solution of the Fokker−Planck equation, predicted that the effects of HIs on rate constants are dependent on spheres' central charges; smaller effects were observed without electrostatic interactions or with electrostatic attraction than with electrostatic repulsion between particles. In our work, however, we considered only attractive and neutral spheres. Both Friedman, and Deutch and Felderhof modeled the interparticle HIs based on the Oseen tensor.[35] The difficulty with this form of the diffusion tensor is that it is not positive-definite for configurations of particles in which the particles are too close to each other[44] and that hydrodynamic interactions are not correctly given by the Oseen formula even for two spheres (unless their separation is large as compared to their radii).[29] In our work, we use the Rotne−Prager−Yamakawa form of the diffusion tensor, which contains first-order corrections for particles of finite sizes[29,30] (while the Oseen diffusion tensor deals with point-like particles) and does not suffer from not being positive-definite for closely positioned particles, which might be the source of discrepancies. However, we should also stress that this description is a pairwise approximation sufficient to describe only far-field HIs.

In case of anisotropic particles (dumbbells), again we observe that association is slowed upon introducing HIs. Interestingly, for anisotropic particles and nonspecific association, we do not observe any dependence of the effects of HIs on particle's charges or ionic strength. However, such dependence manifests itself when specific association (either parallel or perpendicular relative orientation) of dumbbells is considered. We observe that the rates of parallel encounters are less affected by HIs than those of perpendicular ones, which suggests that there is indeed a hydrodynamically preferred orientation of binding partners, an effect that was previously considered by Brune and Kim[23] and by Antosiewicz, Briggs, and McCammon.[24,25] However, strong electrostatic interactions at low ionic strengths and significant excluded volume interactions/steric hindrance may destroy hydrodynamical preferences for particular orientations of binding partners. The maximal magnitude of HI effects on the association rates that we observe is about 30%.

Deutch and Felderhof,[21] and Wolynes and Deutch[22] showed that for spherical particles the effects of HIs increase with decreasing attraction between particles. Fremgen-Kesner and Elcock in their association studies of barnase-barstar[16] observed that the rates of slowly associating protein mutants were more affected by intermolecular HIs than were the rates of fast associating variants. Considering the fact that the increase in ionic strength effectively decreases the electrostatic attraction between the molecules, our results obtained for dumbbells suggest a more complicated behavior for different center-to-center distances, both in parallel and in perpendicular complexes. We clearly see that the HI effects are most pronounced at moderate ionic strengths. Moreover, it is hard to generalize with regard to prediction of the effects of HIs in different systems with electrostatic and excluded volume interactions.

Overall, the effects of HI that were previously estimated for the association of model molecules[20−22,24,25] are mostly of a similar magnitude as the ones obtained here. However, Fremgen-Kesner and Elcock predicted a larger total HI effect on the kinetics of association of barnase and barstar, and they used more complicated models consisting of a larger number of HI centers and charges.

The primary effect of HIs, that is, the slowing of the association, is so far the most general feature observed in the simulations of molecular association and seems to be expected from the physics standpoint; the molecules diffusing in a liquid induce additional liquid fluxes that, in turn, act on other molecules, changing their velocities. The relative diffusion coefficient is reduced, and the decrease in the association rates is observed. However, considering complicated molecular shapes, nonhomogeneous distributions of molecular charges, different intermolecular interactions and their effective range, as well as typical concentrations of molecular species in biological setup, we believe that there is still a need for further theoretical work with different model systems to explain the role of HIs in the association kinetics in biological systems. For example, we have demonstrated that the kinetics of formation of different encounter complexes is affected by HIs differently. We have also shown that steric hindrances and strong electrostatic interactions may destroy hydrodynamic orientational effects; one may relate this result to crowded biological environments in which significant excluded volume effects and nonspecific interactions determine the diffusional behavior of molecules. Simulations of simple systems, as the ones considered in this work, can be treated as an entry point to a more detailed modeling and help in gradually achieving a better understanding of different factors influencing the molecular encounters.

AUTHOR INFORMATION

Corresponding Author

*Phone: +48 22 5540 818. Fax: +48 22 5540 801. E-mail: mdlugosz@cent.uw.edu.pl.

Notes

The authors declare no competing financial interest.

ACKNOWLEDGMENTS

We acknowledge support from National Science Centre (N N519 646640). M.D., P.Z., and J.T. acknowledge support from the University of Warsaw (ICM G31-4). M.D. and J.T. acknowledge support from the Foundation for Polish Science (Focus program). J.T. is supported by the Foundation for Polish Science Team project (TEAM/2009-3/8) cofinanced by the European Regional Development Fund operated within the Innovative Economy Operational Programme and Ministry of Science and Higher Education (N N301 245236). J.M.A. is supported by the University of Warsaw, Faculty of Physics.

REFERENCES

(1) Madura, J. D.; Briggs, J. M.; Wade, R. C.; Davis, M. E.; Luty, B. A.; Ilin, A.; Antosiewicz, J.; Gilson, M. K.; Bagheri, B.; Scott, L.; McCammon, J. *Comput. Phys. Commun.* **1995**, *91*, 57−95.

(2) Davis, M. E.; Madura, J. D.; Luty, B. A.; McCammon, J. *Comput. Phys. Commun.* **1991**, *62*, 187−197.

(3) Gabdoulline, R.; Wade, R. *Methods* **1998**, *14*, 329−341.

(4) Długosz, M.; Antosiewicz, J. M.; Trylska, J. *J. Chem. Theory Comput.* **2008**, *4*, 549−559.
(5) Długosz, M.; Huber, G. A.; McCammon, J. A.; Trylska, J. *Biopolymers* **2011**, *95*, 616−627.
(6) Gabdoulline, R. R.; Wade, R. C. *Biophys. J.* **1997**, *72*, 1917−1929.
(7) Elcock, A.; Gabdoulline, R. R.; Wade, R. C.; McCammon, J. A. *J. Mol. Biol.* **1999**, *291*, 149−162.
(8) Smoluchowski, M. V. *Phys. Z.* **1916**, *17*, 557−571, 585−599.
(9) Smoluchowski, M. V. *Z. Phys. Chem.* **1917**, *92*, 129−168.
(10) Kramers, H. A. *Physica* **1940**, *7*, 284−304.
(11) Debye, P. *Trans. Electrochem. Soc.* **1942**, *82*, 265−272.
(12) Northrup, S. H.; Hynes, J. T. *J. Chem. Phys.* **1979**, *71*, 871−883.
(13) Northrup, S. H.; Allison, S. A.; McCammon, J. A. *J. Chem. Phys.* **1984**, *80*, 1517−1524.
(14) McGuffee, S. R.; Elcock, A. H. *J. Am. Chem. Soc.* **2006**, *128*, 12098−12110.
(15) Gabdoulline, R. R.; Wade, R. C. *J. Am. Chem. Soc.* **2009**, *131*, 9230−9238.
(16) Frembgen-Kesner, T.; Elcock, A. H. *Biophys. J.* **2010**, *99*, L75−L77.
(17) Ermak, D. L.; McCammon, J. A. *J. Chem. Phys.* **1978**, *69*, 1352−1360.
(18) Długosz, M.; Zieliński, P.; Trylska, J. *J. Comput. Chem.* **2011**, *32*, 2734−2744.
(19) Aragon, S. R. *Methods* **2011**, *54*, 101−114.
(20) Friedman, H. L. *J. Phys. Chem.* **1966**, *70*, 3931−3933.
(21) Deutch, J. M.; Felderhof, B. U. *J. Chem. Phys.* **1973**, *59*, 1669−1671.
(22) Wolynes, P. G.; Deutch, J. M. *J. Chem. Phys.* **1976**, *65*, 450−454.
(23) Brune, D.; Kim, S. *Proc. Natl. Acad. Sci. U.S.A.* **1994**, *91*, 2930−2934.
(24) Antosiewicz, J.; Briggs, J. M.; McCammon, J. A. *Eur. Biophys. J.* **1996**, *24*, 137−141.
(25) Antosiewicz, J.; McCammon, J. A. *Biophys. J.* **1995**, *69*, 57−65.
(26) Shushin, A. I. *J. Chem. Phys.* **2003**, *118*, 1301−1311.
(27) Allison, S. *J. Phys. Chem. A* **2006**, *110*, 13864−13867.
(28) Hückel, E. V. *Phys. Z.* **1924**, *25*, 204−2010.
(29) Rotne, J.; Prager, S. *J. Chem. Phys.* **1969**, *50*, 4831−4838.
(30) Yamakawa, H. *J. Chem. Phys.* **1970**, *53*, 436−444.
(31) Smith, E. R.; Snook, I. K.; van Megen, W. *Physica A* **1987**, *143*, 441−467.
(32) Fernandes, M. X.; de la Torre, J. G. *Biophys. J.* **2002**, *83*, 3039−3048.
(33) Harvey, S.; de la Torre, J. G. *Macromolecules* **1980**, *13*, 960−964.
(34) Dickinson, E.; Allison, S. A.; McCammon, J. A. *J. Chem. Soc., Faraday Trans. 2* **1985**, *81*, 591−601.
(35) Kirkwood, J. G.; Riseman, J. *J. Chem. Phys.* **1948**, *16*, 565−574.
(36) de la Torre, J. G.; Bloomfield, V. A. *Biopolymers* **1977**, *16*, 1747−1763.
(37) Bell, G. M.; Levine, S.; McCartney, L. N. *J. Colloid Interface Sci.* **1970**, *33*, 335−359.
(38) Antosiewicz, J. *Biophys. J.* **1995**, *69*, 1344−1354.
(39) Favro, L. D. *Phys. Rev. E* **1960**, *119*, 53−62.
(40) Woessner, D. E. *J. Phys. Chem.* **1962**, *37*, 647−654.
(41) de la Torre, J. G.; Harding, S. E.; Carrasco, B. *Eur. Biophys J.* **1999**, *28*, 119−132.
(42) Mereghetti, P.; Gabdoulline, R. R.; Wade, R. C. *Biophys. J.* **2010**, *99*, 782−3791.
(43) Wieczorek, G.; Zielenkiewicz, P. *Biophys. J.* **2008**, *95*, 5030−5036.
(44) Dames, R. E.; Holland, W. F.; Shen, M. C. *J. Chem. Phys.* **1967**, 2782−2794.